LIGHT EMISSION OF THE PHOTOFRAGMENTS PRODUCED BY PHOTOLYSIS OF AMMONIA AND AMMONIA-d_3 AT 147, 123.6 AND 104.8 NM:

FIRST OBSERVATION OF THE b $^1\Sigma^+$ → X $^3\Sigma^-$ TRANSITION OF NH AND ND

J. MASANET, A. GILLES and C. VERMEIL

Equipe de recherche du CNRS associée à l'E.S.P.C.I., 10 rue Vauquelin, 75231 Paris Cedex 05 (France)

(Received June 6, 1974)

Summary

Excited photofragments are produced by vacuum ultra-violet photolysis of gaseous ammonia and ammonia-d_3. The following transitions have been recorded: $NH_2(ND_2)$ $\widetilde{A}$ $^2A_1$ → $\widetilde{X}$ $^2B_1$ by irradiation with xenon and krypton resonance lamps; NH (ND) c $^1\pi$ → a $^1\Delta$ and b $^1\Sigma^+$ → X^3 Σ^- with the krypton and argon resonance lamps.

This last emission, observed here for the first time, occurs at 471 nm and it leads to the singlet–triplet splitting a $^1\Delta$ − X $^3\Sigma^-$ of NH, with an energy of 1.561 eV (1.565 eV for ND). The rotational temperatures of the c and b excited states of NH and ND radicals have been measured and the primary processes leading to the excited photofragments are discussed.

Introduction

Ammonia photolysis in the gaseous phase has been studied for several decades [1 - 8]. For the last ten years information concerning the excited photofragments has been obtained by optical methods [4 - 8]. There are few studies concerning ND_3 photolysis [3, 4].

In a previous paper [4] we evaluated the kinetic energy of the hydrogen atoms produced.

Here we present results relevant to the observation of emissions during NH_3 and ND_3 photolysis in three spectral ranges: lower than, close to, and higher than their ionization potentials.

The NH b $^1\Sigma^+$ → X $^3\Sigma^-$ radiative transition has been observed for the first time during the course of this photochemical study and we have reported it previously [9]; the experimental value of the energy difference between the triplet $^3\Sigma^-$ ground state and the first singlet excited state a$^1\Delta$ is 1.56 eV.

Spectral and thermodynamic data concerning the ammonia molecule

The ammonia spectrum [10 - 18] is structured at wavelengths longer than 140 nm but becomes very diffuse at $\lambda < 140$ nm so that analysis was possible only for $\tilde{A}$, $\tilde{B}$ and $\tilde{C}$ states [17 - 20]. Douglas [17] showed that the $\tilde{A}$ state predissociates into NH_2 ($\tilde{X}^2B_1$) + H, and that the ground state of ammonia correlates with NH_2 ($\tilde{A}^2A_1$).

The ground state of ammonia belongs to point group C_{3v} (pyramidal symmetry), while the excited states belong to point group D_{3h} [15] (planar symmetry). The ground state of NH_3^+ is also planar (quantum yields of photoionization [3] are 0.4 and 0.42, respectively, for NH_3 and ND_3 at 104.8 nm).

The various thermodynamic data concerning ammonia compiled in 1971 [21], do not assist in deciding which values for $\Delta H_{f(298\ K)}$ (NH_3), (NH) and (NH_2) to choose in order to calculate the thermodynamic thresholds of the two following processes:
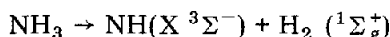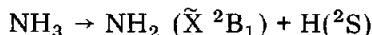
$$NH_3 \rightarrow NH_2\ (\tilde{X}\ ^2B_1) + H(^2S)$$
$$NH_3 \rightarrow NH(X\ ^3\Sigma^-) + H_2\ (^1\Sigma_g^+)$$

TABLE 1

Threshold energies in ammonia decomposition

	E(eV)		
$NH_3 \rightarrow NH(X\ ^3\Sigma^-) + H_2\ (^1\Sigma_g^+)$	3.9	± 0.1	(1)
$\rightarrow NH_2(\tilde{X}\ ^2B_1) + H(^2S)$	4.4	± 0.1	(2)
$\rightarrow NH(a\ ^1\Delta) + H_2(^1\Sigma_g^+)$	5.5	± 0.1	(3)
$\rightarrow NH_2(\tilde{A}^2A_1) + H(^2S)$	5.7	± 0.1	(4)
$\rightarrow NH(b^1\Sigma^+) + H_2(^1\Sigma_g^+)$	6.6	± 0.1	(5)
$\rightarrow NH(A\ ^3\pi) + H_2(^1\Sigma_g^+)$	7.6	± 0.1	(6)
$\rightarrow NH(X\ ^3\Sigma^-) + H(^2S) + H(^2S)$	8.4	± 0.1	(7)
$\rightarrow NH(c\ ^1\pi) + H_2(^1\Sigma_g^+)$	9.3	± 0.1	(8)
$\rightarrow NH(a\ ^1\Delta) + H(^2S) + H(^2S)$	9.9	± 0.1	(9)
$\rightarrow NH_3^+ + e$	10.14 [22]		(10)
$\rightarrow NH(b\ ^1\Sigma^+) + H(^2S) + H(^2S)$	11.1	± 0.1	(11)
$\rightarrow NH(A\ ^3\pi) + H(^2S) + H(^2S)$	12.1	± 0.1	(12)

We have shown [4] that NH_3 photolysis leads to dissociation into NH $(X^3\Sigma^-)$ + H + H. The assumption that 147 nm is the threshold of the reaction, corresponds to the lowest experimental values for ΔH_f (NH) = 78.5 kcal/mol and ΔH_f (NH_3) = —10.5 kcal/mol; NH ($E_{X^3\Sigma^-} - E_{a^1\Delta}$) = 1.56 eV [9].

Thermodynamic thresholds in ammonia decomposition are given in Table 1.

Experimental

Ammonia was obtained from Air Liquide; its purity was 99.6%. The ammonia-d_3 obtained from CEA had a purity of 99.7%. Both were used without further purification.

The experimental apparatus is shown in Fig. 1. Gas at 0.3 Torr pressure (measured by Pirani LKB gauge) flowed at a rate of 0.1 cm^3/s through a cell painted black and equipped with Wood's horns for the elimination of scattered light.
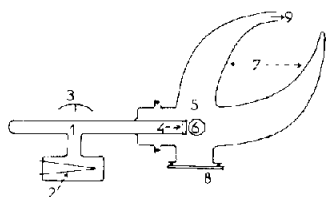

Fig. 1. Experimental apparatus: 1, lamp; 2, titanium wires; 3, microwave power antenna; 4, LiF window; 5, photolysis cell; 6, gas input and pressure measurements; 7, Wood's horns; 8, quartz observation window; 9, gas output and vacuum.

TABLE 2

Wavelengths of the rare gas resonance line emissions

	λ(nm)	E(eV)	Relative intensity (%)
Xe	147	8.45	99
	129.5	9.57	1
Kr	123.6	10.06	80
	116.5	10.65	20
Ar	104.8	11.82	not observed
	106.7	11.62	

The rare gas resonance lamp was filled to 1 Torr pressure with Xe, Kr or Ar, and the gases were purified by heating titanium wires inside the lamp by a 10 A current. Before each experiment, the lamp was tested with a vacuum ultra-violet monochromator (Coderg MSV 102) having a grating of 2400 lines/mm blazed at 121.6 nm.

The wavelengths of the emission lines are shown in Table 2. It was possible to evaluate the relative intensities of the emission lines from xenon and krypton, but the sensitivity of our apparatus rapidly decreased below 115 nm, making it impossible to evaluate the relative intensities of the argon resonance lines.

Emission was observed at right angles to the excitation, through a monochromator (Jobin-Yvon HRP) equipped with a grating of 1221 lines/nm blazed at 500 nm. The dispersion of this apparatus was 1.3 nm/mm. The
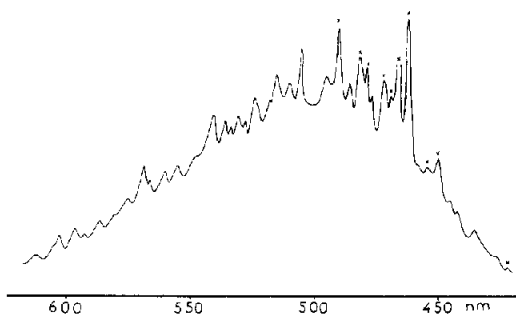
Fig. 2. Emission spectrum NH_2 $\tilde{A}$ $^2A_1$ $\rightarrow$ $\tilde{X}$ $^2B_1$ transition formed during the photolysis of ammonia at 147 nm. * designates Xe scattered lines.

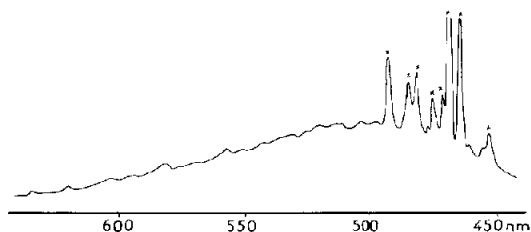Fig. 3. Emission spectrum ND_2 $\tilde{A}$ $^2A_1$ $\rightarrow$ $\tilde{X}$ $^2B_1$ transition formed during the photolysis of ammonia-d_3 at 147 nm. * designates Xe scattered lines.

photomultiplier selected (Hammamatsu R212 UHS) was sensitive in the spectral range 250 - 650 nm and was connected to a picoammeter (Lemouzy PA 15T). The output was recorded on a Graphirac (Sefram).

It is not possible to give a precise value of any quantum yield; by comparison with Okabe and Lenzi's [7] estimation of the NH_2 ($\tilde{A}$ $^2A_1$) quantum yield ($\leqslant 10^{-3}$) during the photolysis of NH_3 in this spectral range, we can infer that our detection system had approximately the same sensitivity for large monochromator slits (1000 μm). But in order to study the rotational structure of these emissions, it is necessary to operate with narrow slits leading to a higher detection threshold.

Results

Xenon resonance lamp (147 and 129.5 nm)

Emission at 129.5 nm is only 1% of the total emission and has been neglected. We observe in Figs. 2 and 3 a diffuse band spectrum lying between 390 nm and the detection limit of the photomultiplier (650 nm). This emission may be assigned [23] to the transition $NH_2 (ND_2)$ $\tilde{A}$ $^2A_1$ $\rightarrow$ $\tilde{X}$ $^2B_1$.

Krypton resonance lamp (123.6 and 116.5 nm)

Three different emissions are observed: (1) a diffuse spectrum identical to the preceding one assigned to $NH_2(ND_2)$ $\tilde{A}$ $^2A_1$ $\rightarrow$ $\tilde{X}$ $^2B_1$; (2) an intense
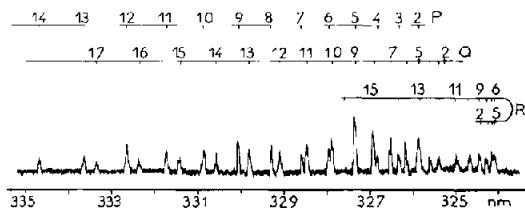
Fig. 4. Emission spectrum in the second order of the 0 - 0 NH c $^1\pi \to$ a $^1\Delta$ transition formed during the photolysis of ammonia by Kr resonance lamp.
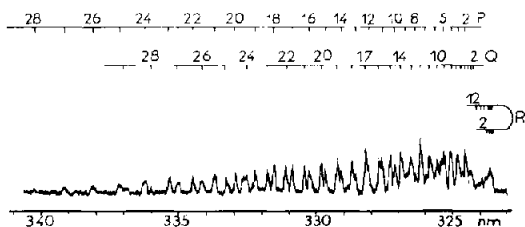

Fig. 5. Emission spectrum in the second order of the 0 - 0 ND c $^1\pi \to$ a $^1\Delta$ transition formed during the photolysis of ammonia-d_3 by Kr resonance lamp.

emission already observed by Becker and Welge [6] for NH_3 lying between 324 and 335 nm (Figs. 4 and 5) which was assigned to the 0 - 0 band of NH (ND) c $^1\pi \to$ a $^1\Delta$. The rotational levels are populated until $J = 17$ for NH and $J = 28$ for ND; (3) a third weaker emission, more intense with ND_3 than with NH_3, composed of an intense central line placed in both cases at 471 nm and surrounded by a fine structure. We have assigned this (see below) to NH(ND) $b^1\Sigma^+ \to X\,^3\Sigma^-$.

Argon resonance lamp (104.8 and 106.7 nm)
(1) Emission of NH_2 (ND_2) $\tilde{A}\,^2A_1 \to \tilde{X}\,^2B_1$ has not been observed; (2) emissions of 0 - 0 (Figs. 6 and 7) and 1 - 0 (Figs. 8 and 9) from the transition NH (ND) c $^1\pi \to$ a $^1\Delta$ occur. Rotational levels are populated until $J = 16$ for NH and $J = 12$ for ND in the (0 - 0) band and until $J = 13$ for NH and $J = 17$ for ND in the (1 - 0) band; (3) emissions of NH(ND) $b^1\Sigma^+ \to X^3\Sigma^-$ become more intense (Figs. 10 and 11).

Spectral analysis of experimental results

NH c $^1\pi \to$ a $^1\Delta$
Spectra of the transition NH(ND) $c^1\pi \to$ a $^1\Delta$ obtained by photolysis at 123.6 nm and 104.8 nm have been analysed, and all the observed lines have been assigned to rotational levels by comparison with the previous assignments for NH [24, 25] and ND [26, 27].
From the intensity distribution of these lines, rotational temperatures could be calculated in the frame of the Born–Oppenheimer approximation, neglecting the vibration–rotation interaction. For this transition, $\pi \to \Delta$
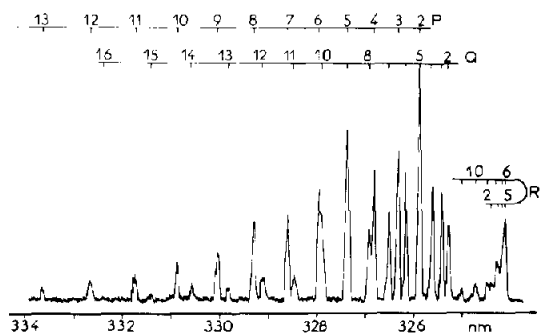
Fig. 6. Emission spectrum in the second order of the 0 - 0 NH c $^1\pi \to$ a $^1\Delta$ transition formed during the photolysis of ammonia-d_3 by Ar resonance lamp.
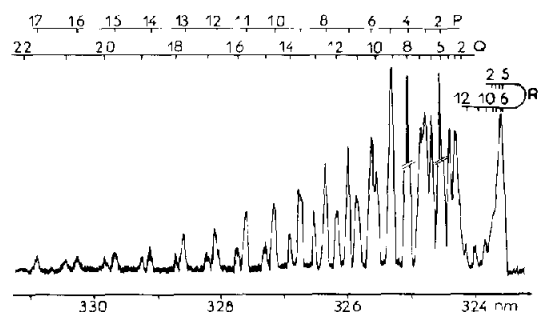
Fig. 7. Emission spectrum in the second order of the 0 - 0 ND c $^1\pi \to$ a $^1\Delta$ transition formed during the photolysis of ammonia-d_3 by Ar resonance lamp.

Fig. 8. Emission spectrum in the second order of the 1 - 0 NH c $^1\pi \to$ a $^1\Delta$ transition formed during the photolysis of ammonia-d_3 by Ar resonance lamp.

($\Delta\lambda = -1$), the intensity distribution is directly linked with the Hönhl–London factors $S_{J'J''}$: the calculation of these factors [28] allows us to obtain the rotational temperature with the following equation:

$$\log \frac{I_{J'J''}}{S_{J'J''} \, \nu_{J'J''}^4} = C_{st} - \left(\frac{E_{J'}}{kT}\right) \log e$$

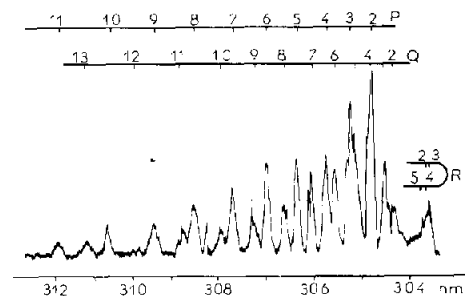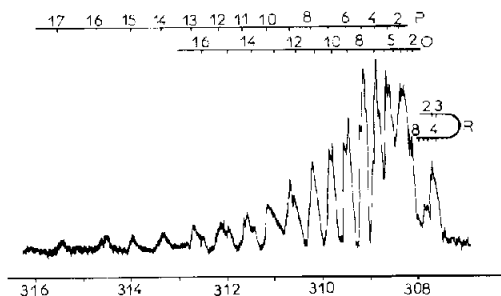where $\nu_{J'J''}$ and $I_{J'J''}$ are respectively the wavenumber and intensity of a $J'J''$

Fig. 9. Emission spectrum in the second order of the 1 - 0 ND c $^1\pi \to$ a $^1\Delta$ transition formed during the photolysis of ammonia-d_3 by Ar resonance lamp.

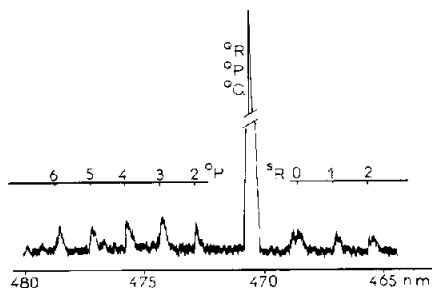Fig. 10. Emission spectrum of NH b $^1\Sigma^+ \to$ X $^3\Sigma^-$ formed during the photolysis of ammonia-d_3 by Ar resonance lines.
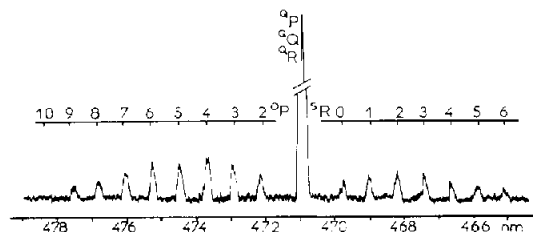
Fig. 11. Emission spectrum of ND b $^1\Sigma^+ \to$ X $^3\Sigma^-$ formed during the photolysis of ammonia-d_3 by Ar resonance lines.

transition, and $E_{J'}$ is the energy of the rotational level J'.

We obtain for each case a straight line whose slope, evaluated by least squares, gives a rotational temperature T. The T values are shown in Table 3.

NH b $^1\Sigma^+ \to$ X $^3\Sigma^-$

As this emission has never been observed before, we shall give a detailed analysis here. The transition is forbidden by the multiplicity rule and therefore its oscillator strength is probably low.

Spectrum analysis

The diagram of this transition is shown in Fig. 12. The spectrum is composed, for NH as for ND, of a very intense central line (Figs. 10 and 11)

TABLE 3

Rotational temperatures of NH(ND)c $^1\pi$ radical formed by photolysis of ammonia and ammonia-d_3 with krypton and argon resonance lines

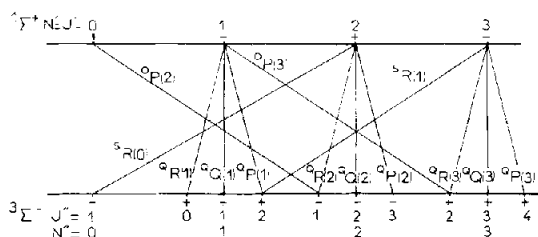|	$\lambda = 123.6$ nm		$\lambda = 104.8$ nm	
	NH	ND	NH	ND
$\nu = 0$	$T = 2745$ K	$T = 2785$ K	$T = 1115$ K	$T = 905$ K
$\nu = 1$	not observed	not observed	$T = 882$ K	$T = 616$ K

Fig. 12. Schematic diagram for the rotational levels of the NH(ND) b $^1\Sigma^+ \to$ X $^3\Sigma^-$ transition.

TABLE 4

Rotational constants of NH(ND)b $^1\Sigma^+$ and NH(ND)X $^3\Sigma^-$

	X $^3\Sigma^-$		b $^1\Sigma^+$	
	NH	ND	NH	ND
B_0 (cm^{-1})	16.3454	8.7822	16.7326	8.3472

with a ^SR branch and a ^OP branch. The three branches ^QP, ^QQ and ^QR overlap each other in the central line. The states b $^1\Sigma^+$ and X $^3\Sigma^-$ are known from work on the transitions c $^1\pi$ H $\to$ b $^1\Sigma^+$ [29, 30] and A $^3\pi \to$ X $^3\Sigma^-$ [31, 32]. The rotational constants already known are shown in Table 4. For both isotopic species, $B_0' - B_0''$ is nearly zero, and consequently all Q branches pile up in a narrow band.

We can calculate the energies of the lines of this transition for NH and ND by taking the $^QQ(0)$ line as the energy origin.

The first ten Q lines overlap within a very narrow range, about 10 cm^{-1}, so that for NH and ND there is only one large intense line in the low resolution spectrum (Table 5). Attempts were made to resolve the central line with a better spectrograph in the Molecular Photophysics Laboratory of Dr. Leach at Orsay. Unfortunately the intensity was too weak and only the Q branch for ND could be observed.

TABLE 5

Measured and calculated lines for NH (ND) b $^1\Sigma^+ \to X\ ^3\Sigma^-$

	NH							ND						
	S_R		Q_R	Q_Q	Q_P	O_P		S_R		Q_R	Q_Q	Q_P	O_P	
N''	calc.	exp.	calc.	calc.	calc.	calc.	exp.	calc.	exp.	calc.	calc.	calc.	calc.	exp.
0	98.53	90						49.63	54					
1	165.12	170		0.17	1.02			89.52	90		0.10	1.29		
2	230.90	244	1.68	0.52	1.48	−96.85	−97	124.96	124	2.05	0.27	1.56	−50.88	−50
3	296.57		2.00	1.05	2.09	−162.10	−155	160.53	160	2.17	0.59	1.98	−86.06	−88
4	362.00		2.56	1.72	2.83	−227.36	−217	195.92	194	2.39	0.91	2.32	−121.01	−121
5	427.65		3.74	2.98	4.15	−290.74	−287	231.43	230	2.86	1.45	2.91	−155.69	−157
6	492.18		4.28	3.59	4.95	−354.89	−349	266.84	263	3.34	1.98	3.54	−190.26	−191
7	556.63		5.50	4.87	6.17	−416.00		302.23		4.09	2.85	4.33	−224.43	−227
8	620.64		6.79	6.22	7.67	−480.44		337.43		4.90	3.48	5.12	−258.40	−263
9	684.18		8.27	7.95	9.38	−542.17		372.62		5.73	4.54	6.14	−292.17	−292
10	745.93		10.11	9.71	11.18	−602.85		407.58		6.78	5.43	7.13	−325.53	−328

Negative signs indicate that the lines are shifted toward the red.

From the observations we have determined the origin of both spectra to be: NH: 471.01 ± 0.25 nm; ND: 470.73 ± 0.13 nm.

Evaluation $\Delta E \ (X \ ^3\Sigma^- - a \ ^1\Delta)$

Observation of this emission permits for the first time the measurement of the triplet–singlet splitting of NH(ND). For the energy difference between the first singlet excited state and the triplet ground state, we obtain the values 1.561 eV for NH and 1.565 eV for ND (Fig. 13). The value for NH is in good agreement with the indirect determination made by Okabe and Lenzi (1.6 eV) and with the theoretical value of 1.47 eV calculated by O'Neil and Schaeffer [33].
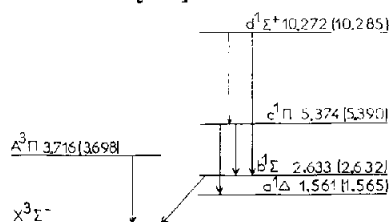

Fig. 13. Energy diagram of NH and ND. The energy values in eV, are the intervals be- tween X $^3\Sigma^-$ ν = 0 level and excited states ν = 0 levels. Values in parenthesis concern ND.

Rotational temperatures

The rotational structure of this emission, observed in the course of the photolysis with Ar lines, allows the rotational temperatures to be evaluated. The Hönhl–London factors for this forbidden transition contain the parallel and perpendicular transition moments (always $\mu_\parallel + \mu_\perp = 1$) and to know these moments it is really necessary to resolve all the Q branches. However, $\mu_\parallel$ and $\mu_\perp$ cancel in the logarithmic equation from which the temperatures are obtained. The Hönhl–London factors are then given by the following equations [34]:

$$S_{J'J''} \ (^OP) = (J + 1)(J + 2)(2J + \tfrac{1}{2})(\mu_\parallel - \mu_\perp)^2$$

$$S_{J'J''} \ (^SR) = J(J - 1)(2J - 1)^{-1} \ (\mu_\parallel - \mu_\perp)^2$$

They are introduced in the logarithmic expression:

$$\log \left(\frac{I_{J'J''}}{S_{J'J''} \ \nu_{J'J''}^4} \right) = - \frac{E_{J''}}{kT} \log e + \text{constant}$$

The analysis performed with only the ^SR and ^OP branches gives for $\nu' = 0$ the following values: T_{NH} = 300 K and T_{ND} = 370 K.

Discussion

NH₂(ND₂) Ã $^2A_1$ radical formation

Okabe and Lenzi [7] have observed the formation of NH$_2$(Ã $^2A_1$) in the course of photolysis of NH$_3$ at wavelengths shorter than 164 nm with a quantum yield $\leqslant 10^{-3}$. This photon energy is the threshold of the NH$_3$

($\tilde{B}$ $^1E''$) state. According to them this state would be predissociated in order to give the $\tilde{A}$ state of NH_2. The present work is in agreement with these results and shows moreover the absence of this dissociation mode at 104.8 nm. The spectrum of the emission NH_2 $\tilde{A}$ $^2A_1$ → $\tilde{X}$ $^2B_1$ perturbed by the Renner–Teller effect [23] is very diffuse and it was impossible to carry out vibrational and rotational analysis.

The dissociation (4) can occur only from two states $^1A_1$ and $^3A_1$ ($^1A_1'$ and $^3A_1'$ in D_{3h} symmetry) because of correlation rules.

The singlet ground state $\tilde{X}$ $^1A_1$ of ammonia directly dissociates into NH_2 ($\tilde{A}$ $^2A_1$) + H, and consequently, a predissociation may occur only through $NH_3(^3A_1)$. The fact that this predissociation is forbidden by multiplicity might explain the low $NH_2(\tilde{A}$ $^2A_1$) quantum yield obtained at 147 and 123.6 nm.

The absence of NH_2 ($\tilde{A}$ $^2A_1$) production at 104.8 nm may be explained in several ways: (a) there may be no intersection between the $^3A_1$ surface and that reached at 104.8 nm; (b) the predissociation may be forbidden by symmetry in addition to the spin interdiction; (c) the predissociation may become negligible as other channels, especially photo-ionization, become available.

NH(ND)c $^1\Pi$ radical formation

NH(c $^1\Pi$) formation by NH_3 photolysis at 123.6 nm has already been observed by Becker and Welge [6]. We confirm this result and, moreover, we observe this radical formation at 104.8 nm. If we refer to Table 1, only the dissociation (8) can be responsible for this radical formation.

As the ammonia molecule is planar in all of its excited states, the ν_2 bending "out of plane" vibration is strongly excited by photon absorption. This excitation mode would lead to rotational motion of NH. In the two cases of argon and krypton photolysis the rotational temperatures are very high. Since the rotational temperature is higher in the krypton case, in the vibrational state reached at 123.6 nm, the ν_2 excitation must be greater than in the state reached at 104.8 nm.

We can perhaps explain the high rotational temperatures observed with the following model. If we consider the planar ammonia molecule as triatomic, taking one NH bond as fixed, then the NH + H_2 dissociation requires the excitation of planar bending vibration. Since the bond length in H_2 is shorter than the H–H distance in NH_3, this bending vibration has to be excited to produce a hydrogen molecule. It is then highly probable that, at the two wavelengths and for the two isotopic compounds, dissociation (8) leads to various population of vibrational levels of $H_2(D_2)$ with different rotational temperature of NH(ND) as measured in the different cases (Table 3).

NH(ND)b $^1\Sigma^+$ radical formation

Two problems arise from the first observation here of this emission: (1) the direct formation of NH(b $^1\Sigma^+$) by photochemical excitation of NH_3 is certainly possible, while, to our knowledge, it does not occur when the

molecule is excited in other ways (electronic impact, flames, discharge, *etc.*); (2) if the photodissociation (5) is responsible for the formation of the radical, we must explain why we do not observe NH(b $^1\Sigma^+$) at 8.45 eV when the thermodynamic photodissociation threshold is 6.6 eV. Also, the process (11) requires a minimum energy of 11.1 eV, 0.5 eV higher than the energy of the second krypton resonance line.

One might be tempted to attribute the formation of NH(b $^1\Sigma^+$) to the dissociation (11) because its energy threshold (11.1 eV) should be higher than the NH$_3$ ionization potential. One would expect that every method of exciting NH$_3$ which could produce ions, would favour ionization against dissociation of a superexcited molecule (NH(b $^1\Sigma^+$) cannot come from NH$_3^+$ because of lack of energy). The uncertainty concerning the heat of formation of NH$_3$ and NH is too great to make a choice between reactions (5) and (11). As NH$_2(\tilde{A}\ ^2A_1)$ would predissociate only into N + H$_2$, and as H$_2$ would dissociate into H + H only if formed in its $^3\Sigma_u^+$ state, whose formation is forbidden from a singlet NH$_3$, the dissociation (11) must directly yield three fragments. The observed low rotational temperatures ($\sim$ 300 K) are not in contradiction with such a dissociation because the excess energy would be easily converted into kinetic energy of the hydrogen atoms.

Unfortunately the radiative lifetime of this NH b $^1\Sigma^+ \rightarrow$ X $^3\Sigma$ transition is not known; being forbidden, its lifetime must be large, higher than that of the allowed c$^1\Pi \rightarrow$ a$^1\Delta$ transition (about 4×10^{-7} s). For the pressure used in this work, thermalization by collision would have to be considered only if the lifetime is longer than 10^{-5} s. If that is the case, and if reaction (5) occurs, a rather high potential barrier would prevent its observation following irradiation at 147 nm (8.45 eV).

Acknowledgements

References

1 U. Schurath, P. Tiedman and R. N. Schindler, J. Phys. Chem., 73 (1969) 457.
2 J. R. McNesby, I. Tanaka and H. Okabe, J. Chem. Phys., 36 (1962) 605.
3 R. L. Lilly, R. E. Rebbert and P. Ausloos, J. Photochem., 2 (1973/74) 49.
4 J. Masanet, J. Fournier and C. Vermeil, Can. J. Chem., 51 (1973) 2946.
5 K. H. Becker and K. H. Welge, Z. Naturforsch., 18a (1963) 600.
6 K. H. Becker and K. H. Welge, Z. Naturforsch., 19a (1964) 1006.
7 H. Okabe and M. Lenzi, J. Chem. Phys., 47 (1967) 5241.
8 K. D. Bayes, K. H. Becker and K. H. Welge, Z. Naturforsch., 17a (1962) 676.
9 A. Gilles, J. Masanet and C. Vermeil, Chem. Phys. Lett., 25 (1974) 346.
10 K. Watanabe, J. Chem. Phys., 22 (1954) 1964.
11 K. Watanabe and S. P. Sood, Sci. of Light, 14 (1965) 36.
12 J. K. Dixon, Phys. Rev., 47 (1935) 711.

13 A. F. B. Duncan, Phys. Rev., 47 (1935) 822.
14 A. F. B. Duncan, Phys. Rev., 50 (1936) 700.
15 A. D. Walsh and P. A. Warsop, Trans. Faraday Soc., 57 (1961) 345.
16 R. S. Mulliken, J. Chem. Phys., 3 (1935) 506.
17 A. E. Douglas and J. H. Hollas, Can. J. Phys., 39 (1961) 479.
18 A. E. Douglas, Discuss. Faraday Soc., 35 (1963) 158.
19 W. R. Harshbarger, J. Chem. Phys., 54 (1971) 2504.
20 W. R. Harshbarger, J. Chem. Phys., 53 (1970) 903.
21 D. R. Stull and H. R. Prophet, JANAF Thermochemical Tables, 2nd Edn, Dow
   Chemical Co., Midland, Mich., 1971.
22 G. R. Branton, D. C. Frost, F. G. Herring, C. A. McDowell and I. A. Stenhouse,
   Chem. Phys. Lett., 3 (1969) 581.
23 G. Dressler and D. A. Ramsay, Phil. Trans. Roy. Soc., A251 (1959) 553.
24 G. Nakamura and T. Shidei, Japan J. Phys., 10 (1934) 5.
25 G. H. Dieke and R. N. Blue, Phys. Rev., 45 (1934) 395.
26 A. Roussel, Thesis, Orsay, France.
27 H. Hanson, I. Kopp, M. Kronekvist and N. Aslund, Arkiv. Fysik., 30 (1965) 1.
28 G. Herzberg, Spectra of Diatomic Molecules, Van Nostrand, Princeton, 1950, p. 208.
29 W. Lunt, R. W. B. Pearse and C. W. Smith, Proc. Roy. Soc., A151 (1935) 602.
30 F. L. Whittaker, J. Phys. (B), 1 (1968) 977.
31 R. N. Dixon, Can. J. Phys., 37 (1959) 1171.
32 P. Bollmark, I. Kopp and B. Rydh, J. Mol. Spectros. 34 (1970) 487.
33 S. V. O'Neil and H. F. Schaeffer III, J. Chem. Phys., 55 (1971) 394.
34 J. K. G. Watson, Can. J. Phys., 46 (1968) 1637.